FROM FUSION TO LIGHT SURFING

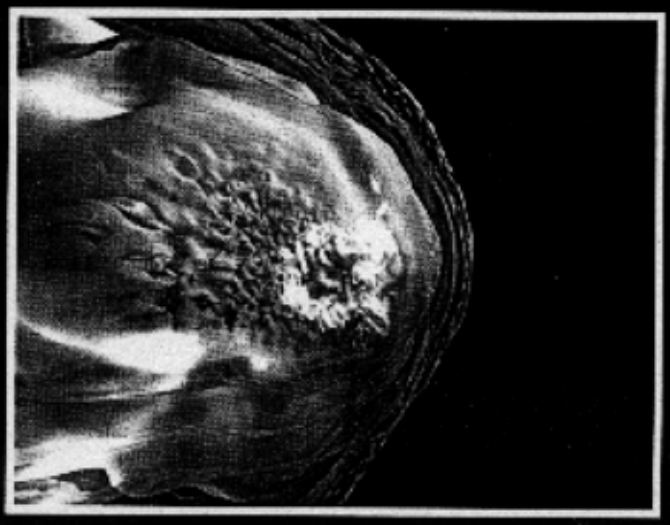

Lectures on Plasma Physics Honoring John M. Dawson

Edited by Thomas Katsouleas

Francis F. Chen
Electrical Engineering Department
University of California, Los Angeles, CA 90024-1594

Double Helix: The Dawson Separation Process

Introduction

In the 35 years during which I have had the pleasure and privilege of being associated with John Dawson, both at Princeton and at UCLA, we have worked on a large variety of subjects in plasma physics. In each case, I found that John's appreciation of experimental realities was remarkable and set him apart from all other theorists. In the 1950s and 1960s, we were concerned with Bohm diffusion, convective cells, drift waves, and minimum-B stabilization. In the 1970s, in connection with the fusion program of EPRI (Electric Power Research Institute), our attention turned to advanced fuels, synchrotron radiation, direct conversion of x-rays, multipole and surmac reactors, laser-heated solenoids, and other alternate concepts. The 1970s also saw the birth of laser fusion (which John foresaw in his Letter on *Giant Pulse Lasers*), parametric instabilities, and experiments to verify these. In the 1980s, John's ideas spawned the UCLA experiments and computations on beat-wave, surfatron, and wake-field accelerators, plasma lenses, electrostatic FEL wigglers, and photon accelerators for frequency up-conversion.

But the project which best illustrates John Dawson's ability to interact with experimentalists is the TRW program on isotope separation, which John initiated and led throughout its life in the period 1973-1986. In an internal TRW report simply entitled "Isotope Separation", dated October 15, 1973, John gave ideas on

several new methods, including the ion cyclotron resonance scheme which eventually grew into a multi-million dollar project. Other physicists had also considered this method, but they never carried out experiments to the point where the real problems arose. John refrained from detailed calculations at first, knowing full well that only experiment could tell him what is important and what is not. Indeed, as the project went on, problem after problem would arise, and John would find the solution. Without his strong physical intuition on which way to go, the project would not have met with the great success that it did.

The PSP (Plasma Separation Process) project at TRW, code-named Task II (there was no such thing as Task I, as far as I know), is probably the most practical project that he and our crew of plasma physicists will ever have worked on. We had to learn the strange terminology of fission: "enrichment", "depletion", "tails", and "SWUs" (separative work units), and deal with such mundane problems as how to keep uranium from flaking off the collectors. Experiments began in small research devices of the Q-machine or filament-discharge type and then moved to M1A, a normal-magnet, ECR-heated device, and to M2A and M2B, two large, dedicated machines with 20-kG superconducting magnets. Finally, the pre-prototype device was constructed and successfully operated. This had a large superconducting magnet around a vacuum chamber with a 1-meter bore (Fig. 1). Plans were made to build a development module in full plant size (Fig. 2), and an entire uranium separation plant would consist of a dozen of these.

The PSP process was, however, in competition with two other advanced isotope separation processes aimed at reducing the cost of producing fissile isotopes below that of the standard gas centrifuge and diffusion plants. One was the MLIS (molecular laser isotope separation) scheme at Los Alamos which used an infrared laser to excite UF_6. The other was the AVLIS (atomic vapor laser isotope separation) scheme at Livermore, which uses a copper-vapor laser to separate uranium and plutonium isotopes. The Dawson process had the advantage that it could be used on any element, not just those with convenient spectral lines. Furthermore, the PSP project succeeded in producing palpable amounts of enriched uranium, while the others had not. In spite of this, a federal review of these projects came out in favor of AVLIS, and funding for the others was discontinued.

The Dawson process has a promising future nonetheless. The versatility of ICRH separation can be applied to such present uses as betavoltaic batteries for space vehicles and such future uses as tailoring of fusion wall materials, disposal of radioactive waste, and tagging with C^{13}. But the greatest potential is for producing medical isotopes. Indeed, TRW has recently provided the medical profession with 40 g of Pd^{102} (a 20,000 dose supply), which is used for radiation treatment of prostate cancer; and we can expect that the Dawson process will be of help to thousands of people requiring medical treatment in the near future.

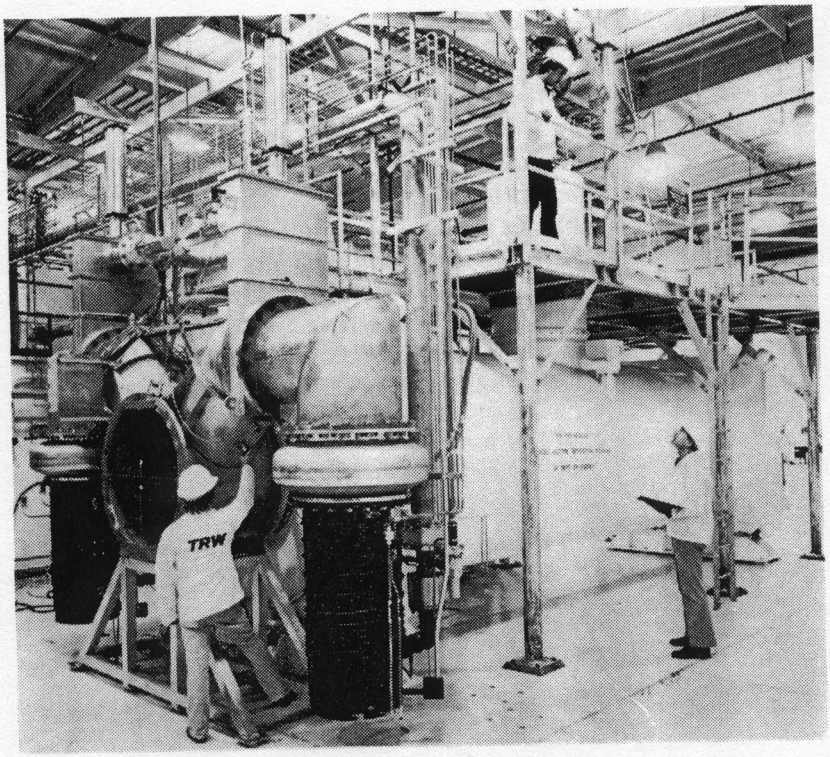

FIGURE 1 The TRW Pre-prototype Facility [*TRW Quest*, Vol. 6, No. 1, Winter 1982/83].

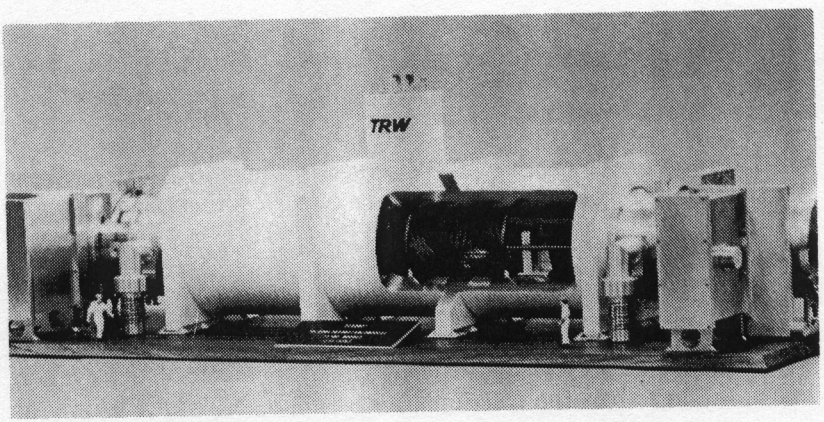

FIGURE 2 Model of full scale module [*TRW Quest*, Vol. 6, No. 1, Winter 1982/83].

The Early Stages

Natural uranium has a majority isotope U^{238} and a minority isotope U^{235} with an abundance of 0.7%. For use in reactors, the U^{235} must be enriched to above 3%. In the Dawson process (Fig. 3), a plasma containing natural uranium is produced in a strong magnetic field, and a radiofrequency field is applied at a frequency which resonates with the cyclotron motion of the minor species but is out of synch with the major species. The minor ions are then accelerated ("spun up") into large orbits and can be separated in a collector at the end away from the source. The collector, which will be described later, yields batches of depleted and enriched uranium. If necessary, the material can be run through again for further enrichment. The SWUs are computed from a formula which accounts for not only the throughput and enrichment, but also the depletion of the tails.

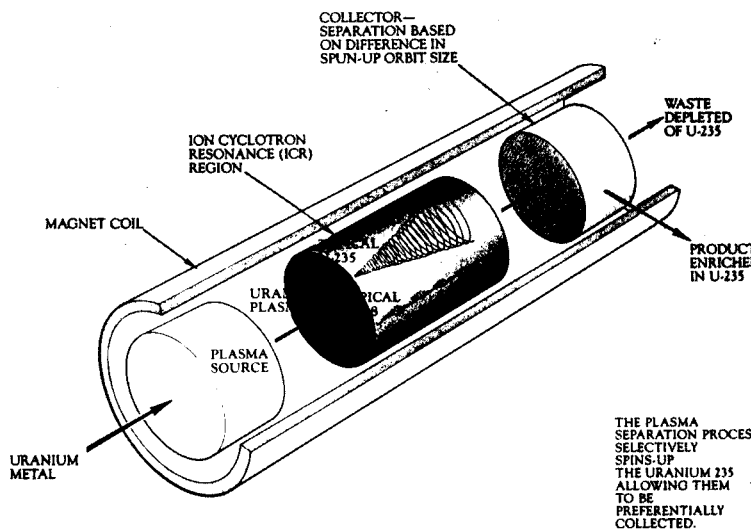

FIGURE 3 Diagram of the process [TRW brochure, *Advanced Isotope Separation Program: Plasma Separation Process for Uranium Enrichment*, August 1981].

The basic principles were outlined in a report by Fried, Dawson and Arnush[1] in 1975. In this paper, it was pointed out that the width of the cyclotron resonance had to be less than the fractional mass difference, which is only about 1% in uranium. That meant that the field uniformity $\Delta B/B$, the collision probability ν/Ω_c, and the transit time loss $v_{||}/\Omega_c L$ all had to be less than 1%. Several methods for separating the spun-up species from the cold species were proposed:

magnetic mirrors which worked on the difference in pitch angle, collectors which worked on the difference in diffusion rates, chemical reactions which depended on the temperature, and Venetian blind collectors which scraped off the large-orbit ions. Eventually the last of these was adopted. The plasma method had the advantage over the Calutron and similar devices in that space charge was automatically canceled, and the method could be used on elements other than uranium – in fact, more easily, because of the larger mass differences.

The first calculations showing the feasibility of the PSP included papers by Fried, Dawson, and Bollens[2], Wilcox[3], Coroniti and Fredricks[5], Fried[6], and Caponi[7]. Proof-of Principle experiments were done in Q-machines by A.Y. Wong et al. and in filament discharges by Stenzel et al.[8,9]. The main experimental results were summarized in a *Phys. Rev. Letter* by Dawson et al.[10], one of the few published papers by the TRW group. In this paper, data were given showing resonant acceleration of K, Ne, Cl, A, and Xe isotopes, as well as enrichment of potassium from a K^{41}/K^{39} ratio of 0.07 to a ratio of 4. The Q machine data in Fig. 4 show a clear separation of the K^{39} and K^{41} peaks. Most of the work was done in filament discharges such as that shown in Fig. 5. The rf voltage was applied across split endplates, an excitation method called "direct drive". Fig. 6 shows the separation of Xe peaks in this device.

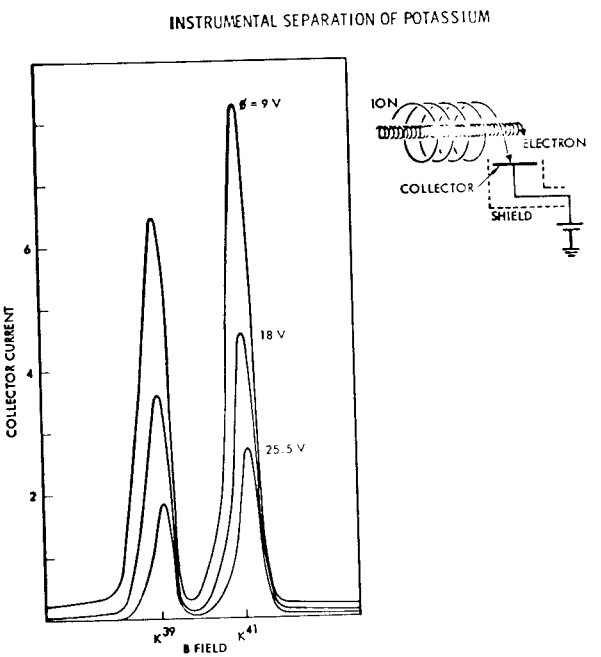

FIGURE 4 Cyclotron resonance peaks in potassium [Ref. 10].

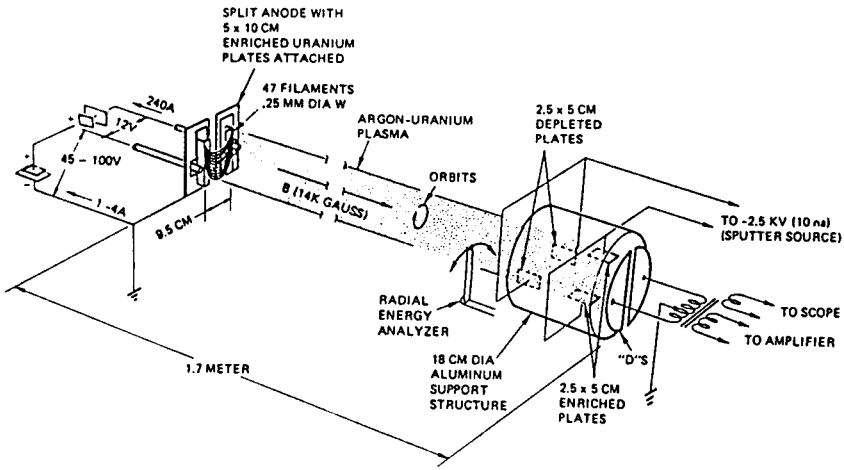

FIGURE 5 Filament discharge with direct drive "dees" [TRW Status Report DSP-192, Sept. 1976].

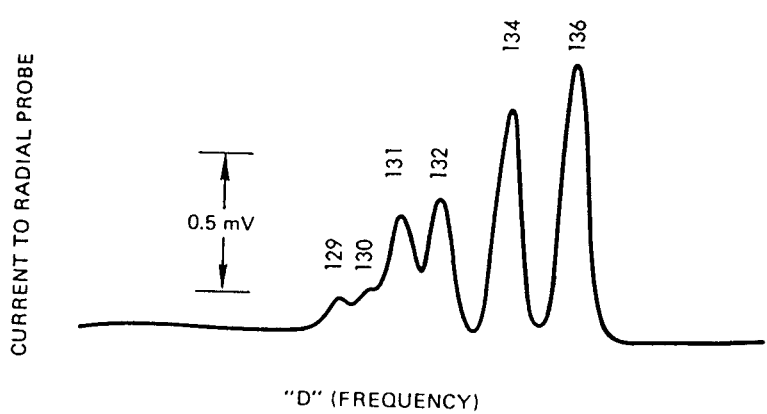

FIGURE 6 Separation of xenon cyclotron resonance peaks [Ref. 10].

Measurements of the rf field inside the plasma, shown in Fig. 7, were made in an argon plasma with a 5% krypton additive and a nitrogen impurity. It is seen that only a broad minimum of the rf E-field occurs near the argon resonance, but a sharp minimum occurs near the resonance of the minor species. The current of fast ions shows peaks near the krypton and nitrogen resonances.

These results can be understood from a simple treatment of two-ion plasmas. There is a frequency, called the two-ion hybrid frequency, at which the two ion fluids oscillate out of phase in such a way as to cancel each other's space charge. This frequency was given long ago by Buchsbaum[11]:

$$\omega^2 = \Omega_1\Omega_2 \frac{\alpha_1\Omega_2 + \alpha_2\Omega_1}{\alpha_1\Omega_1 + \alpha_2\Omega_2} \quad . \tag{1}$$

Here Ω_1, Ω_2 and α_1, α_2 are the cyclotron frequencies and relative densities of the major and minor species, respectively. In the limit of small α_2, the two-ion hybrid frequency approaches the cyclotron frequency of the minor species. The smaller the density of the minors, the larger must their excursions be in order to cancel the space charge of the majors. To achieve large velocities for species 2, the frequency must be close to their cyclotron resonance. This explains the sharp increase in dielectric constant near Ω_2 in Fig. 7. The two-ion resonance is ideal for isotope separation because it is self-adjusting: the minor ion velocity is larger, the smaller its concentration.

Eq. (1) holds only for $k_{||} = 0$. If the propagation $\mathbf{k}$ has a sufficiently large component along $\mathbf{B}$, the electrons can move along the field to cancel the space charge, and the frequency will deviate significantly from that in Eq. (1). Fig. 8 shows ω/Ω_1 as a function of $k_{||}/k_{\perp}^{11}$. At vanishingly small $k_{\perp}$, the two roots are the lower hybrid and the two-ion hybrid oscillations. When $k_{||}/k_{\perp}$ is of order $(m/M)^{\frac{1}{2}}$, there are two electrostatic ion cyclotron waves, one near Ω_1 and one near Ω_2. For $k_{||}/k_{\perp} > 1$, these become pure cyclotron oscillations. The waves near Ω_2 are shown on an expanded scale in Fig. 9; it is seen that the frequency actually differs from Ω_2 in the three regions of $k_{||}$, depending on the density and temperature of the minor species. The aforementioned advantage of the two-ion hybrid can be utilized if $k_{||}/k_{\perp}$ can be kept below $(m/M)^{\frac{1}{2}}$ by the excitation mechanism, or else simple acceleration at Ω_2 can be applied.

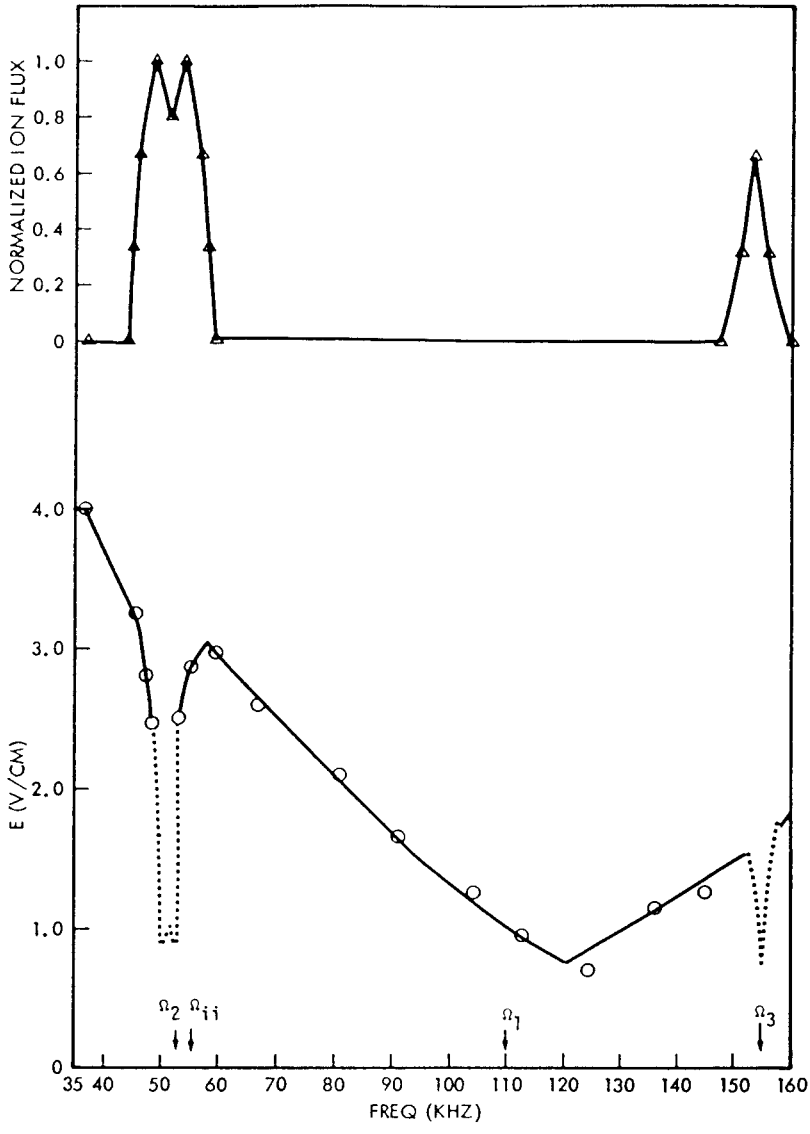

FIGURE 7 Fast ion flux (top) and E-field (bottom) in Ar-Kr plasma, as a function of frequency, in a 3-kG magnetic field. Here Ω_1, Ω_2, and Ω_3 are, respectively, the argon, krypton, and nitrogen cyclotron resonance frequencies, and Ω_{ii} is the two-ion resonance frequency [Ref. 9].

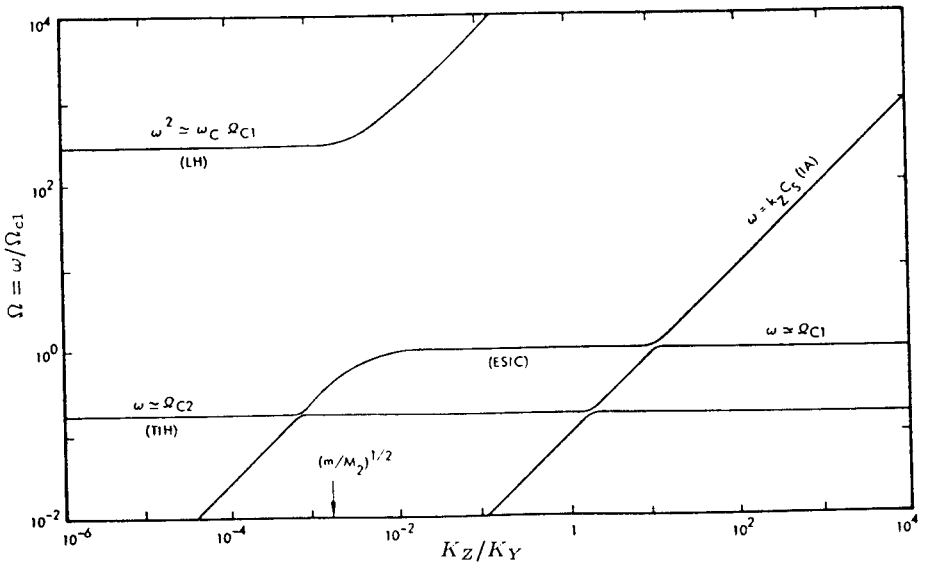

FIGURE 8 Dispersion curves for electrostatic waves in a two-ion plasma [Ref. 11].

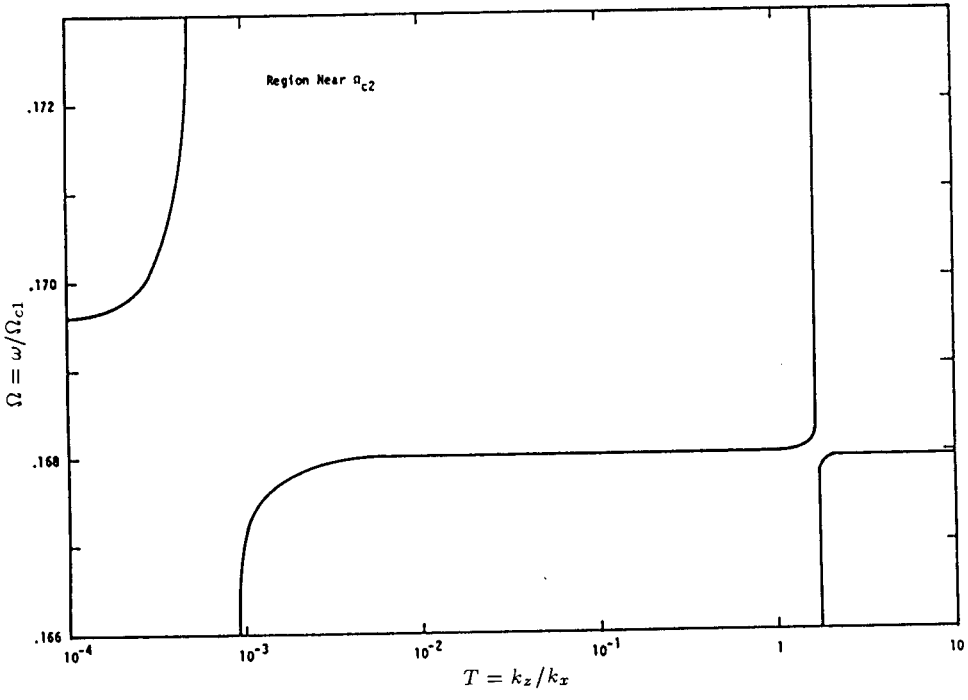

FIGURE 9 The region of Fig. 8 near the minor resonance, shown on an expanded vertical scale [Ref. 11].

Experiments with Uranium

The serious work on separating uranium was done in three large machines with uniform magnetic fields provided by superconducting magnets. One was devoted to plasma measurements, a second to uranium collections, and the third, the large pre-prototype device, was run under production conditions. The different parts involved in each apparatus are shown schematically in Fig. 10. In the source region, uranium atoms were sputtered into the discharge from a negatively biased plate faced with natural uranium. These are ionized by ECRH at 28 GHz. The discharge is started with argon, but the argon can be valved off later to obtain a pure uranium plasma. The plasma streams into the excitation region of uniform field, where a helical antenna generates a left-hand polarized field ($\sim$ 120 kHz, $\sim$ 2V/cm) resonant with U^{235}. These ions are spun up to an energy of about 500 eV. The U^{238} ions, being nonresonant, are alternately accelerated and decelerated, ending up with an effective temperature of about 100 eV. The electrons cool away from the source to a temperature of about 1 eV. With neutral U pressures of 1-50 mtorr, plasma densities up to 1.6×10^{12} cm^{-3} could be produced. The ions stream into the collector region, where a "Venetian blind" array of fences scrapes off the hot ions, which have an average Larmor radius of 2.7 cm, and allow the cold ions ($r_L \sim 1.2$ cm) to pass through to the tails plate. The separation is further aided by a bias voltage. The solid products and tails are removed periodically in batches.

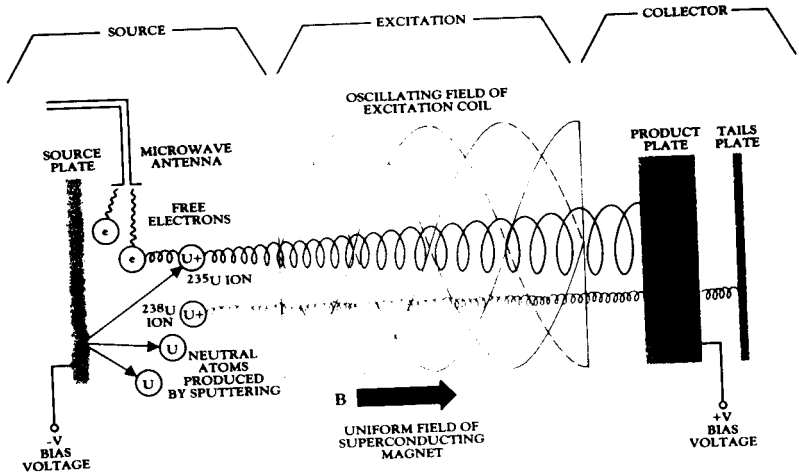

FIGURE 10 Schematic of the apparatus used for separation of uranium [*TRW Quest*, Vol. 6, No. 1, Winter 1982/83].

Each part of the process had problems which had to be solved, and we discuss each of these in turn.

Field uniformity. By purchasing large-diameter superconducting solenoids, it was easy to keep the magnetic field sufficiently constant and uniform. The price that had to be paid was accessibility. Diagnostics had to be introduced from the ends, and an array of long probe shafts protruded from the collector end of the machines.

Vapor source. Sputtering was found to be the most convenient way to introduce uranium atoms. The mounting and cooling of the uranium plates were not severe problems, and control over the neutral pressure and electron temperature could be achieved by varying the bias voltage.

Plasma production. After experimentation with various sources, it was decided that the best method was electron cyclotron resonance heating using the 28 GHz sources developed for ECRH in magnetic fusion. The magnetic field was expanded into a conducting cavity containing the typical curved surface where $\omega = \omega_c$, and the neutrals from the sputter plate were effectively ionized by the microwave power. There were, however, hotspots in the cavity which created ripples in density and potential which propagated along the field lines and could be seen with probes. These inhomogeneities caused broadening of the ion resonance and could have been removed by stirring the microwaves or modulating the frequency. However, this was never done because this was not the limiting effect. In high-power operation, the usual waveguide problems of windows and arc detection had to be overcome.

Wave excitation. Direct drive using split endplates causes the potential on the field lines terminating in each segment to fluctuate at the rf frequency. However, the rf field is not uniformly distributed over the plasma volume. Therefore, inductive drive was used, with an antenna inside the vacuum chamber. The antenna consisted of two intertwined helices (hence the title of this paper) of water-cooled copper, fed 90° apart in phase so as to excite a field in the ion gyration direction (Fig. 11). Extensive calculations of the field pattern inside the plasma produced by antennas of different pitch angles, numbers of wavelengths, and end rings were carried out by McVey[12,13]. Measurements confirmed these field patterns.

Species control. Doubly ionized uranium could have been spun up by the second harmonic of the rf field, but it would not have been collected properly and would have decreased the enrichment factor. The ionization potentials 6.2 and 11.8 eV for U^+ and U^{++} are sufficiently far apart that the population of U^{++} could be held down by running at the low T_e of 1 eV.

Ion acceleration. Aside from transit time, the factor limiting the energy to which the minority ions could be spun up was collisions, both Coulomb and hard-body. For this very practical application, the hard-body cross section had to be known very accurately. Throughout the project, extensive computer modeling accompanied the experiments, and the enrichment ratios and yields were predicted for the actual

operating conditions. The success of differential ion heating was reported to the public by Romesser et al.[14].

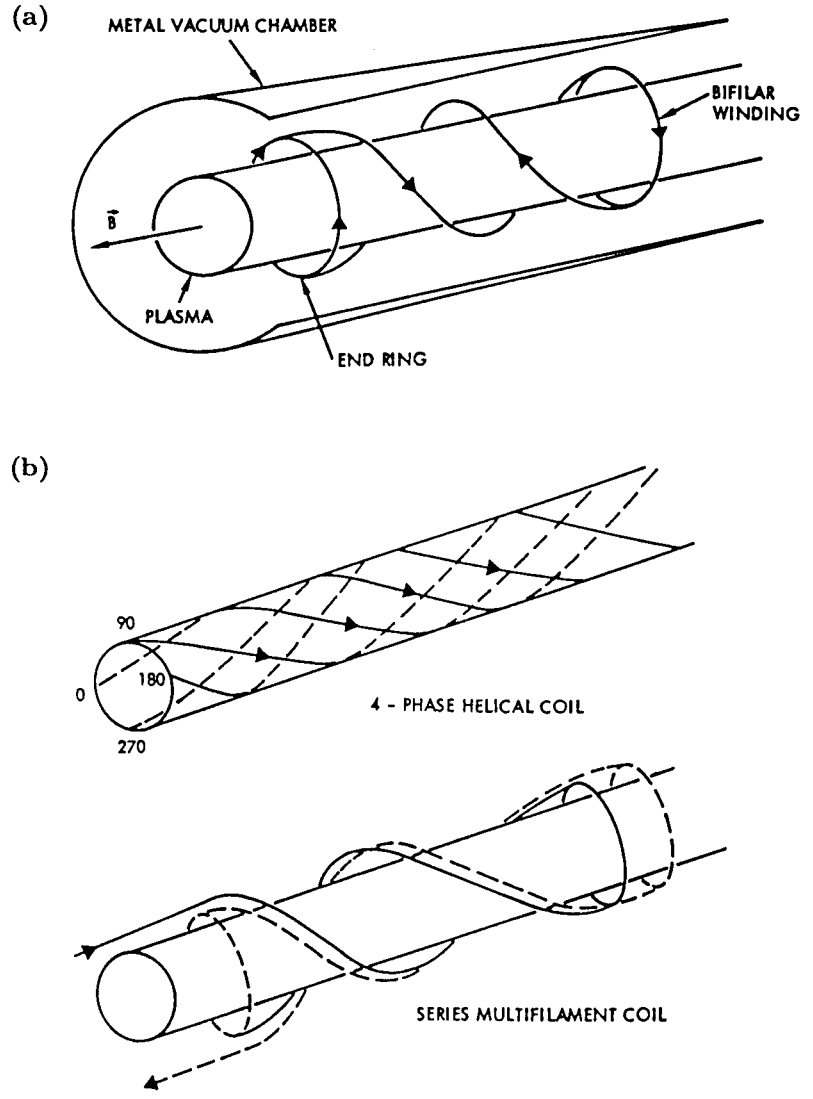

FIGURE 11 Examples of helical windings [Ref. 13]: **(a)** filamentary current model; **(b)** helical coil configurations

Product collection. The Venetian-blind collectors consisted of plates shielded by fences which prevented small Larmor radius ions from striking the plate (Fig. 12). The length of the plates and the height of the fences were adjusted to optimize the enrichment.

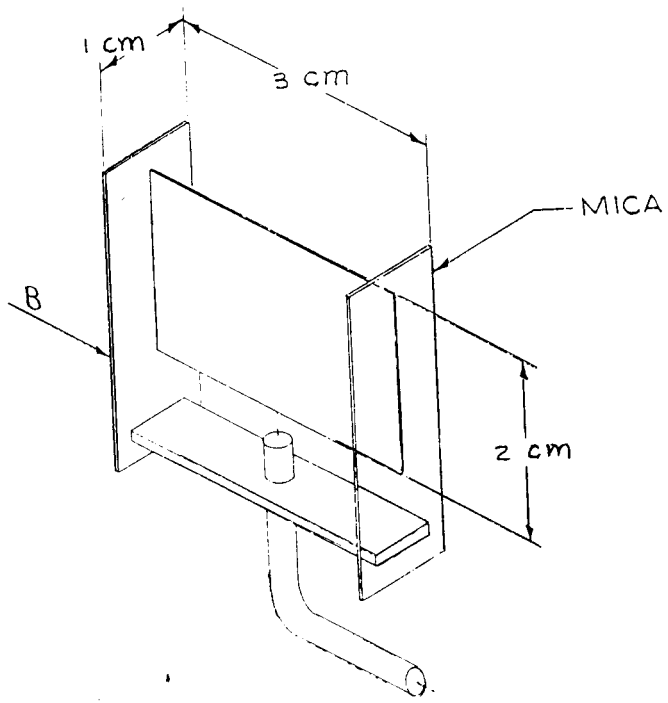

FIGURE 12 Schematic of a collector [TRW Monthly Report DSP-113, July 1976].

Diagnostics. An impressive array of diagnostics was used to characterize the plasma parameters. Standard single and double Langmuir probes, microwave interferometers, and optical spectrometers gave information on density and density fluctuations in space and time, electron temperature, and ion species. In the later stages, laser induced fluorescence was used to measure ion velocities. To measure dc and rf space potential, and hence electric field, an emissive probe was developed[15], which is heated by electron bombardment and switched electronically to a high-impedance load for measurement of the floating potential while the tip is still hot.

The main diagnostic, however, was the radial energy analyzer (REA), shown in Fig. 13, consisting of a biased collector recessed in a cylindrical tube. The tube scraped off the electrons so that only ions were collected, and the ion temperature could be obtained by varying the bias. The space-charge limit to the operation of REAs was found[16] to be $n = 2.5\,\mathrm{E(keV)}/d(mm)^2 \times 10^{10}\ \mathrm{cm}^{-3}$, where n is the density of minority ions inside the tube. This limit was not serious, and the REA was used daily to check the efficiency of acceleration. The space charge surrounding scrape-off devices like REAs and mass spectrometer probes[17] is an interesting problem (Fig. 14).

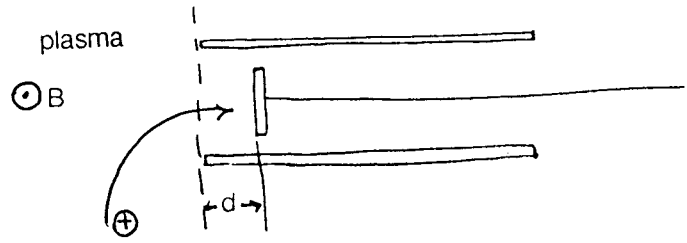

FIGURE 13 A radial energy analyzer

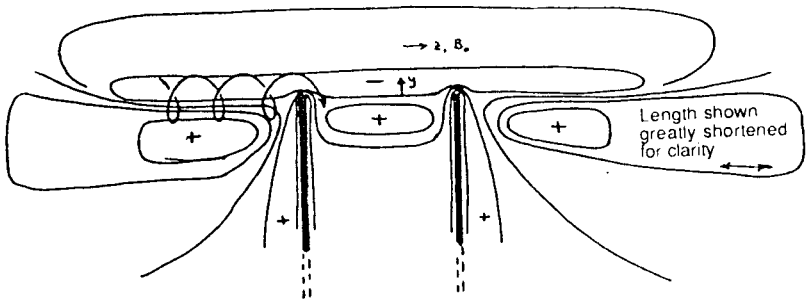

FIGURE 14 Space charge around a radial energy analyzer [Ref. 16]

Interesting Physics Questions

Research on this project turned up some rather interesting problems in basic plasma physics.

Space charge. From the beginning, those who had had experience with the Calutron expressed great skepticism over whether or not this scheme could circumvent the problems of space charge that had plagued previous attempts at plasma isotope separation. Of course, ordinary space charge had been fully accounted for in solving for the fields using standard plasma theory, but what about the edges? Would the large-orbit ions stick out radially past the well confined electron column so that they could not be neutralized? Would the column the rotate like a crankshaft? This question was answered in two ways. Kindel et al.[18] did a numerical simulation with boundaries, and Chen[19] included drift wave terms in treating the two-ion hybrid wave in a plasma with a density gradient. In each case, the effect of space charge was found to be negligible.

Endplate boundary conditions in direct drive. We see from Fig. 8 that the two-ion hybrid can be excited only if $k_{||}$ is extremely small, usually smaller than can be accommodated within a machine with a length of several meters. From Q-machine work, it is known[20] that the sheaths on the endplates can act as insulators, so that waves can have parallel wavelengths much longer than the plasma length. However, the solution for the collisional plasmas of Q-machines would not work for the more collisionless plasmas produced by ECRH. The electron parallel velocity is then limited by both resistivity and electron inertia, terms which are 90° out of phase. Is there a similar effect in this case, making it possible for $k_{||}$ to take on small values? We found[21] that, indeed, this was possible, but that the standing waves in this case are not pure cosines but are strange-looking cosines with a phase shift that varies with axial position.

Diagnostics with the two-ion hybrid. Early experiments with direct drive by the TRW group[22] showed that the two-ion resonance, as evidenced by the peak in the REA current, occurred at a frequency that varied with the density ratio α_2/α_1, as predicted by Eq. (1). This was difficult to understand, because the plasma was not long enough to let $k_{||}/k_{\perp}$ be less than $(m/M)^{\frac{1}{2}}$, and the frequency should have been much higher than that given by Eq. (1). Applying the sheath theory of Ref. 21 did not bring the theoretical curves within the experimental error (Fig. 15). We found, however, that agreement could be achieved if one accounted for the damping of the wave between the two endplates (Fig. 16). Once this is understood, detection of the two-ion hybrid excited by split endplates becomes a simple and useful technique to measuring the density of impurities in a plasma[22].

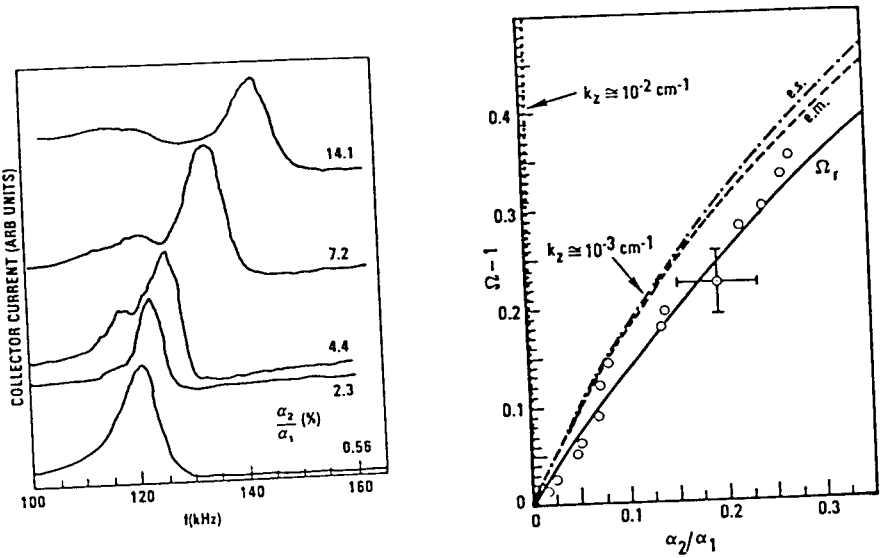

FIGURE 15 Measurements of the frequency shift from the minor species cyclotron resonance, as a function of impurity concentration. The solid line is the prediction of the Buchsbaum formula. The other theoretical curves correspond to cases (A) and (B) in Fig. 16.

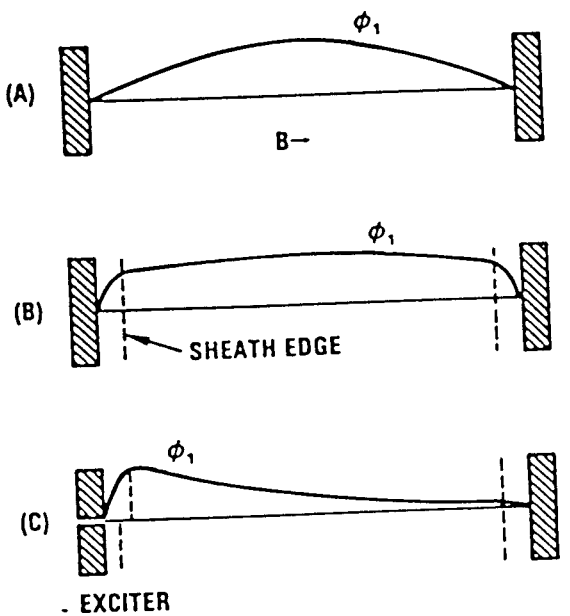

FIGURE 16 Behavior of the axial amplitude variation in (A) a standing wave with no sheath, (B) a standing wave with insulating sheaths, and (C) a damped wave excited by a split plate at one end.

Field enhancement with Type III antennas. The helical antennas used in this project were a variation of the Nagoya Type III antenna[23]. John Dawson was the first to point out the physical reason for the superior performance of such antennas. Fig. 17 shows the essential elements of the antenna, which are finite $k_{||}$ and $k_{\perp}$ and current elements along the direction of $\mathbf{B_0}$. As $\mathbf{J}$ increases, a field $E_{||}$ is induced in the plasma by the field B_1. This causes electrons to flow along each field line until they meet other electrons coming from the adjoining half-wavelength.

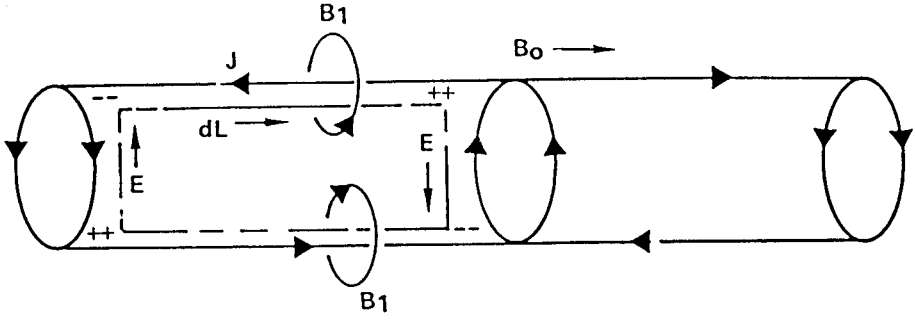

FIGURE 17 Mechanism of the Nagoya Type III antenna [Ref. 24].

Electrostatic charges then build up, giving rise to an electrostatic E-field. Since the plasma is a good conductor, the electrostatic $E_{||}$ field builds up until it cancels the electromagnetically induced $E_{||}$ field, so that the total $E_{||}$ is zero. The same space charge creates a field $E_{\perp}$, since $k_{\perp}$ is finite. This $E_{\perp}$ field is in the same direction as that induced by the transverse legs of the antenna but can be much larger. Electrons cannot move across $\mathbf{B}$ to short out this transverse field, so it can penetrate as far as an ion skin depth c/Ω_{pi}. Thus, the Type III mechanism not only converts the electromagnetic signal into an internal electrostatic field but also amplifies the induced field. In slab geometry (Fig. 18), the enhancement factor is found[24] to be approximately $(k_{\perp}/k_{||})^2$; furthermore, this factor is valid right through the ion cyclotron resonance. Detailed treatment of the cylindrical case was given by McVey[13] with essentially the same result, and experimental confirmation of field enhancement was reported by Tang et al.[25].

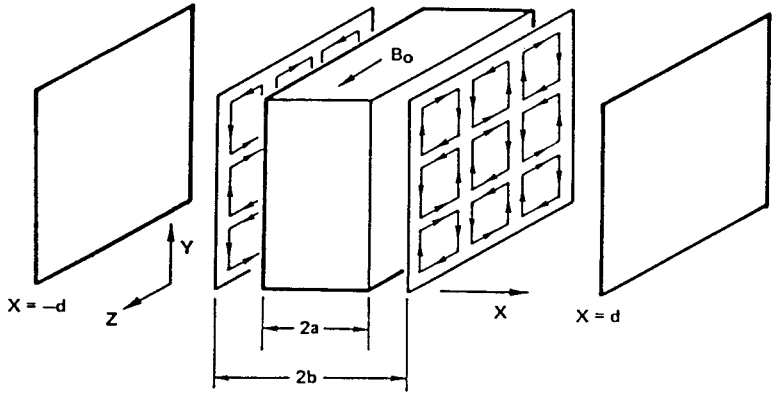

FIGURE 18 Geometry used for calculating the enhancement factor [Ref. 24].

Bandwidth broadening. Though the enrichment of U^{235} in uranium was successfully achieved in macroscopic amounts, the temperature ratio of the resonant and non-resonant species was not as high as theory predicted. The primary cause for this was traced to broadening of the resonance by random pulses in plasma potential. Typical pulses and the broadening of the rf spectrum that they produced are shown in Fig. 19. The pulses are field aligned, with transverse dimensions of the order of the ion gyroradius, and occur at random intervals averaging 1 msec when the rf excitation is strong. The pulses are always positive and have amplitudes up to 40V, much higher than the electron temperature. These observations could be explained qualitatively by a model in which the rf ponderomotive force caused unstable growth of density filaments[26]. This model was criticized, however, because it didn't fit all the data, and another mechanism based on phase-bunching of the ion orbits was proposed by M. Mussetto. John Dawson had a third idea connected with ion viscosity. Unfortunately, the project was stopped before this interesting effect was resolved. The resolution could have had ramifications in other applications of ICRF.

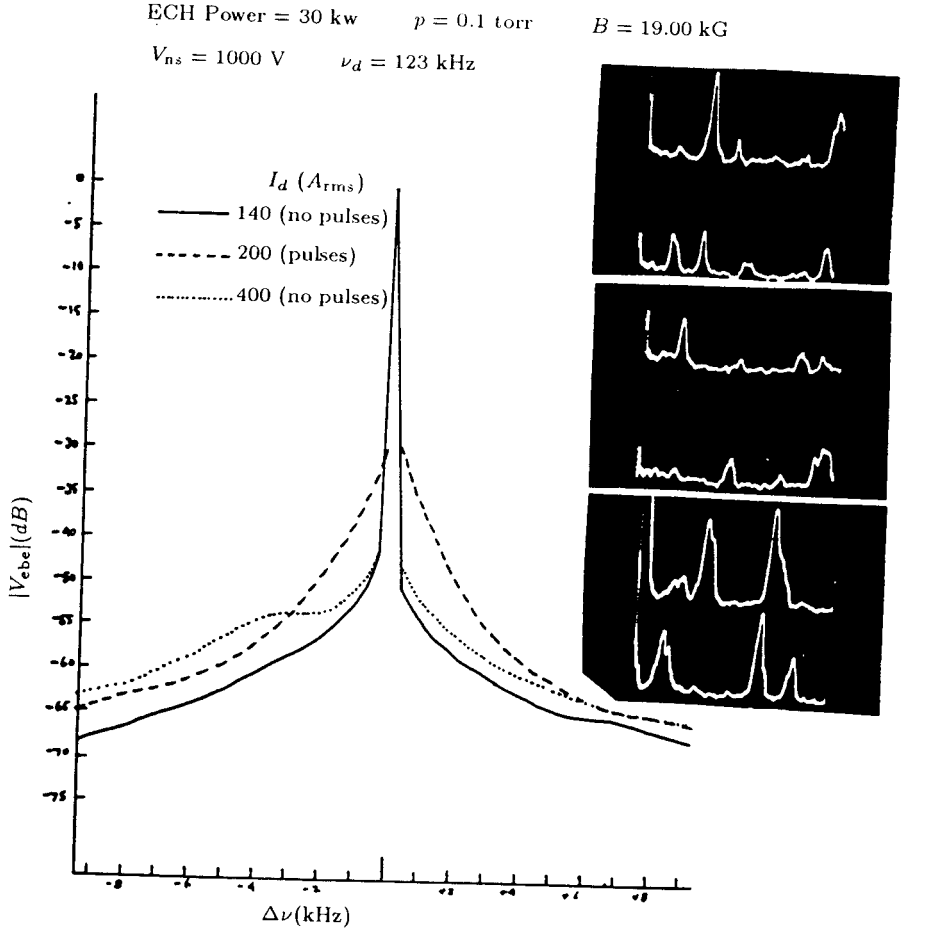

GURE 19 Frequency spectrum of the rf field showing the broadening caused by random pulses in plasma potential (inset).

Acknowledgments

Because this was a classified project, the references in this paper are skewed toward the work that saw the light of day in either published papers or unclassified reports. The success of the project was due to a large number of dedicated physicists and engineers, only some of whose names can be found in the references quoted here. Tom Romesser was the chief scientist, and Larry Harnett the chief engineer. Steve Korn was the program manager, and Sol Rocklin his deputy. Umbrellas were provided by Don Arnush, who headed the plasma efforts at TRW, and his boss, Pete Staudhammer. But it was John Dawson who thought up the idea in the first place and carried it over the many obstacles.

References

1. B.D. Fried, J.M. Dawson, and D. Arnush, "The Dawson Separation Process", TRW Report 29160-6001-RU-00 (Aug. 1975).
2. B. Fried, J. Dawson, and R. Bollens, "Magnetic Pumping and Ion Cyclotron Resonance Heating for a Multi-species Plasma", TRW Report (unnumbered) (Oct. 1974).
3. T.J. Wilcox, "Selective Ion Heating by Cyclotron Resonant Pumping in a Multicomponent Plasma", TRW Report 99900-7781-RU-00 (Dec. 1974).
4. F.V. Coroniti and R.W. Fredricks, "Charge-exchange Collisions in the Dawson Separation Process", TRW Report 29160-6029-RU-00 (Mar. 1976).
5. R.W. Fredricks, "Effect of Collisions on Line Broadening in Electromagnetic Cyclotron Resonance Device", TRW Report 99994-6291-RU-00 (Feb. 1975).
6. B.D. Fried, "Transit-time Effects in Ion Cyclotron Resonance Heating of Multi-Species Plasmas", TRW Report Task II-THA-01 (Dec. 1977).
7. M. Zales Caponi, "Single Particle Resonances in a Nonuniform Electric Field Produced by Direct Excitation of End Electrodes", TRW Report (unnumbered) (Feb. 1977).
8. R.L. Stenzel and J.T. Tang, "Electrostatic Excitation of Ion Cyclotron Resonances", TRW Report 99994-6324-RU-00 (Mar. 1976).
9. J.T. Tang, R.L. Stenzel, and H.C. Kim, "RF Electric Fields in Ion Cyclotron Excitation of Multispecies Plasma", TRW Report Task II-2120 (Jan. 1979); *Phys. Fluids* **22**, 1907 (1979).
10. J.M. Dawson, H.C. Kim, D. Arnush, B.D. Fried, R.W. Gould, L.O. Heflinger, C.F. Kennel, T.E. Romesser, R.L. Stenzel, A.Y. Wong, and R.F. Wuerker,

"Isotope Separation in Plasmas by Use of Ion Cyclotron Resonance", *Phys. Rev. Letters* **37** 1547 (1976).

11. F.F. Chen, "DSP Theory for Experimentalists", TRW Report Task II-1359 (Mar. 1978).
12. B.D. McVey, "Electric Field Patterns for Multiphase Helical Coils", TRW Report Task II-2584 (Sept. 1979).
13. B.D. McVey, "Excitation Theory of the Inductive Drive", TRW Report Task II-2740 (Jan. 1980).
14. T.E. Romesser, *Bull. Amer. Phys. Soc.* **24** 1052 (1979), papers 7B2, 4F8-11.
15. L.L. Higgins, *Bull. Amer. Phys. soc.* **23**, 803 (1978), paper 4F13.
16. F.F. Chen, "Space Charge in Radial Energy Analyzers", TRW Report Task II-1712 (1976).
17. F.F. Chen, "Operation of Mass Spectrometer Probes", TRW Report Task II-2235 (Mar. 1979).
18. J.M. Kindel, A.T. Lin, J.M. Dawson, and R.M. Martinez, "Nonlinear Effects of Ion Cyclotron Heating of Bounded Plasmas", *Phys. Fluids* **24**, 498 (1981).
19. F.F. Chen, "The Two-Ion Hybrid Wave in an Inhomogeneous Plasma", TRW Report PSP-5056 (1982).
20. F.F. Chen, *Plasma Physics* **7**, 399 (1965).
21. F.F. Chen, "Axial Eigenmodes of Long-$\lambda_{||}$ Waves in Plasmas Bounded by Sheaths", *Phys. Fluids* **22**, 2346 (1979).
22. F.F. Chen, G. Dimonte, T. Christensen, G.R. Neil, and T.E. Romesser, "Use of the Two-Ion Hybrid as an Impurity Diagnostic", *Phys. Fluids* **29**, 1651 (1986).
23. T. Watari et al., *Phys. Fluids* **21**, 2076 (1978).
24. F.F. Chen, "Radiofrequency Field Enhancement Near Ion GyroResonance", TRW Report Task II-3552 (Jan. 1981).
25. J.T. Tang, M. Mussetto, B. McVey, D. Dixon, and T. Romesser, *Bull. Amer. Phys. Soc.* **24**, 992 (1979), paper 4F11.
26. F.F. Chen, "An ICRF-driven Inverse Filamentation Instability", TRW Report PSP-TW-348 (1984).